RNA (2001), *7*:524–536. Cambridge University Press. Printed in the USA.

Generating new ligand-binding RNAs by affinity maturation and disintegration of allosteric ribozymes

GARRETT A. SOUKUP,[1,2] ELIZABETH C. DEROSE,[1] MAKOTO KOIZUMI,[1,3] and RONALD R. BREAKER[1]

[1]Department of Molecular, Cellular and Developmental Biology, Yale University, New Haven, Connecticut 06520-8103, USA

ABSTRACT

Allosteric ribozymes are engineered RNAs that operate as molecular switches whose rates of catalytic activity are modulated by the binding of specific effector molecules. New RNA molecular switches can be created by using "allosteric selection," a molecular engineering process that combines modular rational design and in vitro evolution strategies. In this report, we describe the characterization of 3′,5′-cyclic nucleotide monophosphate (cNMP)-dependent hammerhead ribozymes that were created using allosteric selection (Koizumi et al., *Nat Struct Biol*, 1999, *6*:1062–1071). Artificial phylogeny data generated by random mutagenesis and reselection of existing cGMP-, cCMP-, and cAMP-dependent ribozymes indicate that each is comprised of distinct effector-binding and catalytic domains. In addition, patterns of nucleotide covariation and direct mutational analysis both support distinct secondary-structure organizations for the effector-binding domains. Guided by these structural models, we were able to disintegrate each allosteric ribozyme into separate ligand-binding and catalytic modules. Examinations of the independent effector-binding domains reveal that each retains its corresponding cNMP-binding function. These results validate the use of allosteric selection and modular engineering as a means of simultaneously generating new nucleic acid structures that selectively bind ligands. Furthermore, we demonstrate that the binding affinity of an allosteric ribozyme can be improved through random mutagenesis and allosteric selection under conditions that favor tighter binding. This "affinity maturation" effect is expected to be a valuable attribute of allosteric selection as future endeavors seek to apply engineered allosteric ribozymes as biosensor components and as controllable genetic switches.

Keywords: aptamer; catalytic RNA; effector; hammerhead; in vitro selection; molecular recognition

INTRODUCTION

Allosteric ribozymes are an engineered class of RNA catalysts whose activities are regulated by the binding of specific effector molecules (Soukup & Breaker, 1999a, 2000a, 2000b). These effector-modulated catalysts have been engineered to recognize and respond to numerous effector types including a variety of small molecules (Tang & Breaker, 1997a, 1997b, 1998; Araki et al., 1998; Koizumi et al., 1999; Robertson & Ellington, 1999; Soukup & Breaker, 1999b, 1999c; Jose et al., 2001; Robertson & Ellington, 2000; Soukup et al., 2000) and oligonucleotides (Porta & Lizardi, 1995; Kuwabara et al., 1998; Robertson & Ellington, 1999, 2000; Hamada et al., 2000; Komatsu et al., 2000; Tanabe et al., 2000). Allosteric ribozymes have vast potential to serve either as molecular switches for the precision control of cellular processes or as biosensors for the detection of analytes. Ribozymes with allosteric properties already have been shown to control gene expression in vivo (Kuwabara et al., 1998; Hamada et al., 1999; Tanabe et al., 2000) and to function in a prototype RNA array as biosensor elements for the detection of target compounds in complex chemical solutions and biological samples (Seetharaman et al., 2001).

Allosteric ribozymes require an arrangement where an allosteric domain changes shape upon binding an

Reprint requests to: Ronald R. Breaker, Department of Molecular, Cellular and Developmental Biology, Yale University, New Haven, Connecticut 06520-8103, USA; e-mail: ronald.breaker@yale.edu.

[2]Present address: Department of Biomedical Sciences, Creighton University School of Medicine, 2500 California Plaza, Omaha, Nebraska 68178, USA.

[3]Present address: Sankyo Co., Ltd. 2-58, Hiromachi 1-Chrome, Shinagawa-Ku, Tokyo 140-8710, Japan.

effector, which in turn modulates the function of an adjoining catalytic domain (Soukup & Breaker, 2000b). These constructs can be created by using modular rational design strategies (Tang & Breaker, 1997a; Soukup & Breaker, 1999b) that suitably integrate preexisting ligand-binding aptamers (Gold et al., 1995; Chow & Bogdan, 1997; Osborne & Ellington, 1997; Famulok, 1999) and preexisting ribozymes (Eckstein & Lilley, 1996; Carola & Eckstein, 1999). However, rational design strategies used in conjunction with in vitro selection techniques (Williams & Bartel, 1996; Breaker, 1997) typically yield allosteric catalysts with superior ligand-dependent function (Soukup & Breaker, 1999c; Robertson & Ellington, 2000).

Allosteric ribozymes presumably can utilize as effectors virtually any chemical entity that can influence the structure of RNA upon binding. However, strategies for the development of ligand-dependent catalysts that rely exclusively on the integration of preexisting aptamers fall short when no apparent strategy for integrating aptamer and ribozyme exists, or particularly when no aptamer is easily attainable. We have recently described a process termed "allosteric selection" that can be used to generate allosteric ribozymes with new effector specificities from a random-sequence RNA population (Koizumi et al., 1999). Specifically, the RNA population was created by replacing stem II of the self-cleaving hammerhead ribozyme (Carola & Eckstein, 1999) with a 25-nt random-sequence domain. Ribozymes were isolated by the iterative selection and amplification protocol only if they contained unique ligand-binding sites derived from the random-sequence region that also modulated self-cleavage activity. Using this allosteric selection process, various hammerhead ribozymes that require cGMP, cCMP, or cAMP as effector molecules were isolated simultaneously from the same initial population (Koizumi et al., 1999). Although these allosteric ribozymes exhibit excellent molecular discrimination capabilities and kinetic properties, the affinity of each catalyst for its cognate effector is relatively poor. Furthermore, little can be inferred from the primary sequence alone regarding the structural organization and allosteric function of each effector-binding domain.

In this study, we have further analyzed the cGMP-, cCMP-, and cAMP-dependent ribozymes using a variety of techniques to understand better the structure, function, and limitations of these allosteric catalysts. Artificial phylogeny data and mutational analysis are used to determine the secondary structure of each effector-binding domain. Structural analyses demonstrate that the effector-binding domains, when removed from the context of their respective allosteric ribozymes, exhibit ligand-binding properties. Therefore, the effector-binding domains of catalysts developed using allosteric selection can be engineered as functionally distinct ligand-binding RNAs. Furthermore, we demonstrate that the affinity of an allosteric ribozyme for its cognate ligand can be improved through random mutagenesis and selection under more stringent reaction conditions. These investigations also provide insight into a general mechanism of allosteric regulation for the cNMP-dependent ribozymes.

RESULTS

Structural characteristics of cNMP-dependent ribozymes

The structural features of each effector-binding domain from the cGMP-1, cCMP-1, and cAMP-1 ribozymes (Koizumi et al., 1999) were identified using three strategies. First, the Zuker (1989) RNA MFOLD algorithm[1] was used to identify possible base-paired regions. Second, artificial phylogeny data were generated for each ribozyme by mutagenizing the effector-binding domain and by using allosteric selection to isolate sequence variants that retain ligand-dependent self-cleavage activity. Third, directed mutational analysis was used to validate the secondary structure models for each ribozyme and to evaluate the necessity of certain sequence components within each effector-binding domain.

The effector-binding domain of cGMP-1 is proposed to contain two stem elements (IIa and IIb) in addition to stem II of the hammerhead ribozyme domain (Fig. 1A). The artificial phylogeny of cGMP-dependent ribozymes demonstrates that nucleotides comprising the unpaired segments in the putative three-stem junction are highly conserved whereas nucleotides within each loop of stems IIa and IIb are less well conserved (Fig. 2B). Two variants (7 and 10) have mutations that are not consistent with the formation of a three-stem junction in stem II of cGMP-1. In contrast, covariations observed for base-paired nucleotides within stem IIa (variant 3) or stem IIb (variant 4) are consistent with the proposed secondary structure model derived by the structure-prediction algorithm.

Mutational analysis was used to examine the important structural features of the cGMP-binding domain in greater detail (Fig. 1C). A single guanosine substitution within the putative three-stem junction of cGMP-1 mitigates effector dependence (variant *a*). Interestingly, the position of guanosine substitution tolerates any of the other 3 nucleotides without loss of allosteric function as demonstrated by the artificial phylogeny data (Fig. 1B). Variant *a* has an abnormally high rate of RNA cleavage in the absence of cGMP relative to the parent cGMP-1 RNA (data not shown). Therefore, we speculate that the guanosine substitution might lend stability to stem II through the formation of an additional G-C base pair, thereby stabilizing the active form of the variant ribozyme even in the absence of effector. This would

[1]The RNA M-FOLD algorithm can be accessed on the internet (http://bioinfo.math.rpi.edu/~mfold/rna/form1.cgi).

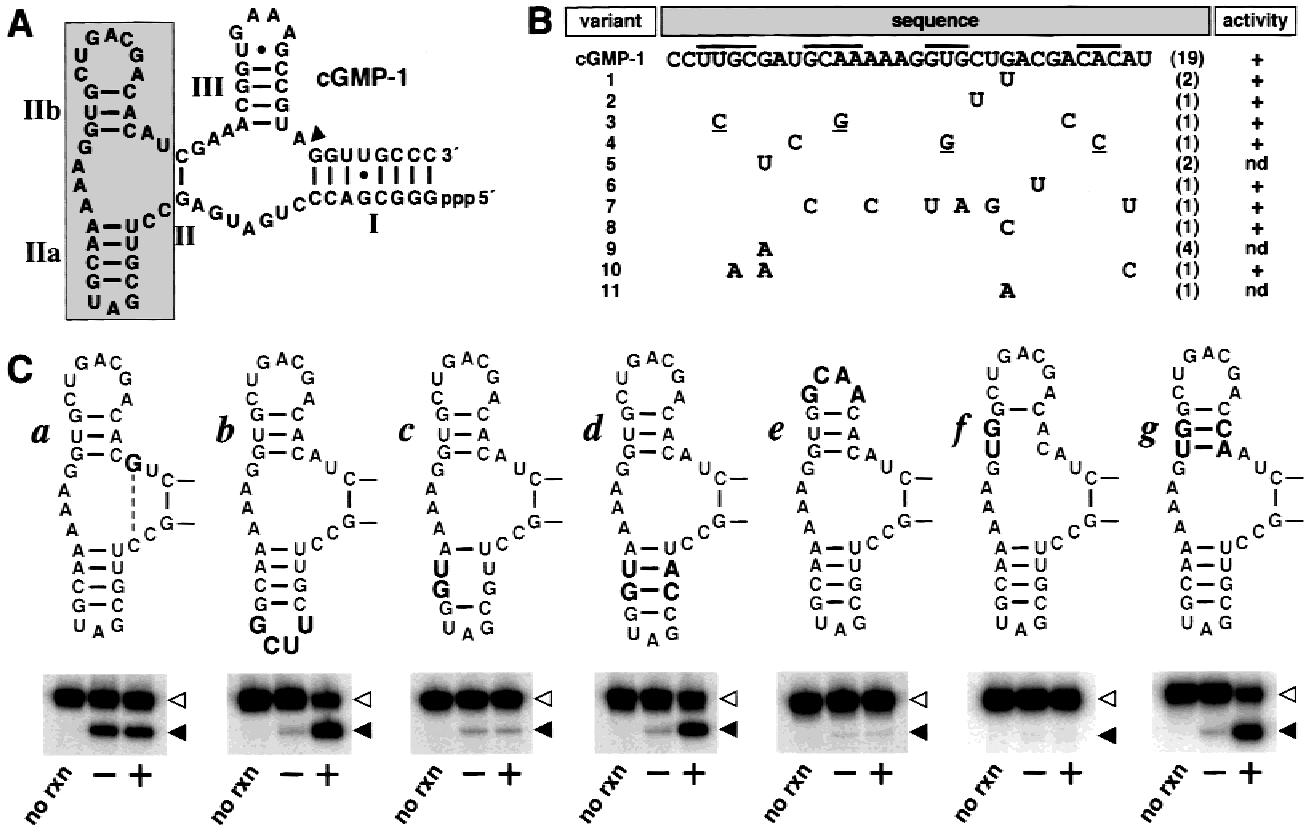

FIGURE 1. Secondary-structure analysis of a cGMP-dependent ribozyme. **A:** Proposed secondary structure of cGMP-1. Denoted are stems I, II, and III of the hammerhead ribozyme domain (Hertel et al., 1992), the site of catalytic cleavage (arrowhead), and stems IIa and IIb of the cGMP-binding domain (shaded box). **B:** Artificial phylogeny of cGMP-1. Shown are sequence variants of the proposed effector-binding domain of cGMP-1 that were identified by allosteric selection for ligand-dependent function from a degenerate population of ribozymes. The mutations acquired by each variant are depicted relative to the parent construct. Mutations that maintain base pairing within the putative stem regions (indicated by bars) are underlined. Numbers in parentheses indicate the frequency of occurrence for each variant. Variants that retain cGMP-dependent activity under selection conditions are indicated (+). The activity of certain variants was not determined (nd). **C:** Mutational analysis of cGMP-1. Shown are sequence variants of cGMP-1 (stem II region only) that were used to examine different structural aspects of the ligand-binding domain. Sequence changes relative to the parent cGMP-1 construct are denoted (bold). For each variant *a–g*, the self-cleavage activity in the absence (−) or presence (+) of 500 μM cGMP under selection conditions is depicted as an autoradiogram of internally ^{32}P-labeled RNAs separated by denaturing 10% PAGE. Lanes containing unreacted ribozyme are indicated as "no rxn." Open and filled arrowheads denote the precursor ribozyme and 5′-cleavage product, respectively.

also be consistent with a mechanism of allosteric activation for cGMP-1 that involves ligand-dependent stabilization of the G-C base pair comprising stem II (Ruffner et al., 1990; Fedor & Uhlenbeck, 1992), whose stability is critical for ribozyme function (Tuschl & Eckstein, 1993; Long & Uhlenbeck, 1994).

Other mutational analyses either support the formation of stems IIa and IIb or indicate the importance of their corresponding loop sequences in cGMP-1 function (Fig. 1C). For example, replacement of loop IIa with a tetraloop sequence does not deleteriously affect cGMP-dependent function (variant *b*), suggesting that the precise composition of loop IIa is largely inconsequential with respect to either ligand recognition or allosteric function of cGMP-1. In contrast, mutations that disrupt stem IIa formation are observed to disrupt cGMP-dependent self-cleavage activity (variant *c*), and compensatory mutations that restore stem IIa formation restore cGMP-dependent function (variant *d*). These data demonstrate that stem IIa is a requisite structural component of the cGMP-binding domain. The impact of mutations in loop IIb and stem IIb were similarly examined (variants *e–g*). Both stem IIb formation and loop IIb sequence are necessary for ligand recognition or allosteric function of cGMP-1. The latter observation indicates that loop IIb might interact with the core of the effector-binding domain or otherwise be involved in the allosteric conversion between inactive and active states of the cGMP-dependent ribozyme.

The effector-binding domains of the cCMP-1 and cAMP-1 ribozymes were similarly characterized using RNA MFOLD, artificial phylogeny analysis, and mutational analysis (Figs. 2 and 3, respectively). For cCMP-1 (Fig. 2A), the artificial phylogeny reveals that both the

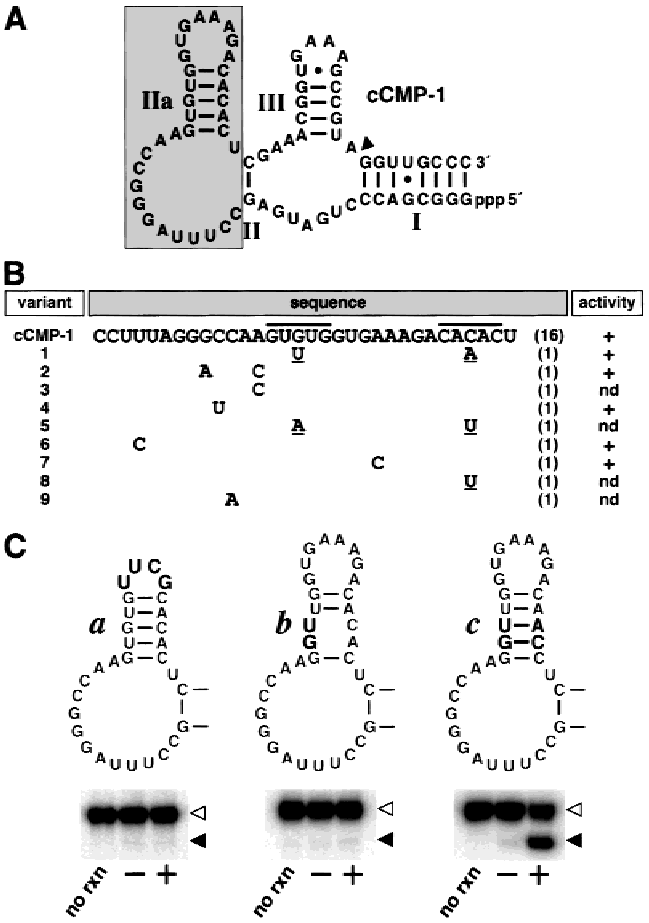

FIGURE 2. Secondary structure analysis of a cCMP-dependent ribozyme. **A:** Proposed secondary structure of cCMP-1. Denoted are stems I, II, and III of the hammerhead ribozyme domain, the site of catalytic cleavage (arrowhead), and stem IIa of the cCMP-binding domain (shaded). **B:** Artificial phylogenetic analysis of cCMP-1. Shown are sequence variants of cCMP-1 that were identified by allosteric selection for ligand-dependent function from a degenerate population of ribozymes. Annotations are as described for Figure 1B. **C:** Mutational analysis of cCMP-1. Shown are sequence variants of cCMP-1 (stem II region only) that examine different structural aspects of the ligand-binding domain. Annotations are as described for Figure 1C.

stem and loop elements of IIa are highly conserved components of the ligand-binding domain. For example, three variants exhibit mutations in stem IIa sequence that are consistent with base-pair formation (Fig. 2B). Mutational analyses further demonstrate the necessity of stem and loop IIa in cCMP-1 function (Fig. 2C). Although truncation of loop IIa disrupts cCMP-dependent self-cleavage activity (variant *a*), mutations in stem IIa that prohibit ligand-dependent ribozyme function (variant *b*) can be offset by compensatory mutations that restore function (variant *c*). These data demonstrate that stem IIa formation and loop IIa sequence are required for the allosteric function of cCMP-1. For cAMP-1 (Fig. 3A), the artificial phylogeny (Fig. 3B) and mutational analyses (Fig. 3C) similarly demonstrate a critical role for stem and loop IIa in allosteric function.

In both the cCMP-1 and cAMP-1 ribozymes, the 5′ bulge between stems II and IIa varies somewhat in primary sequence (Figs. 2B and 3B, respectively). However, the bulge loop in the ligand-binding domain of cCMP-1 demonstrates higher sequence conservation in its 5′ region, whereas the 3′ region of the corresponding bulge loop in cAMP-1 is more conserved. Although the secondary structure model for the ligand-binding domain of cCMP-1 is similar to that for cAMP-1, there exist distinct differences in the primary sequences that likely contribute to the discrete effector-binding specificities observed for each ribozyme (Koizumi et al., 1999).

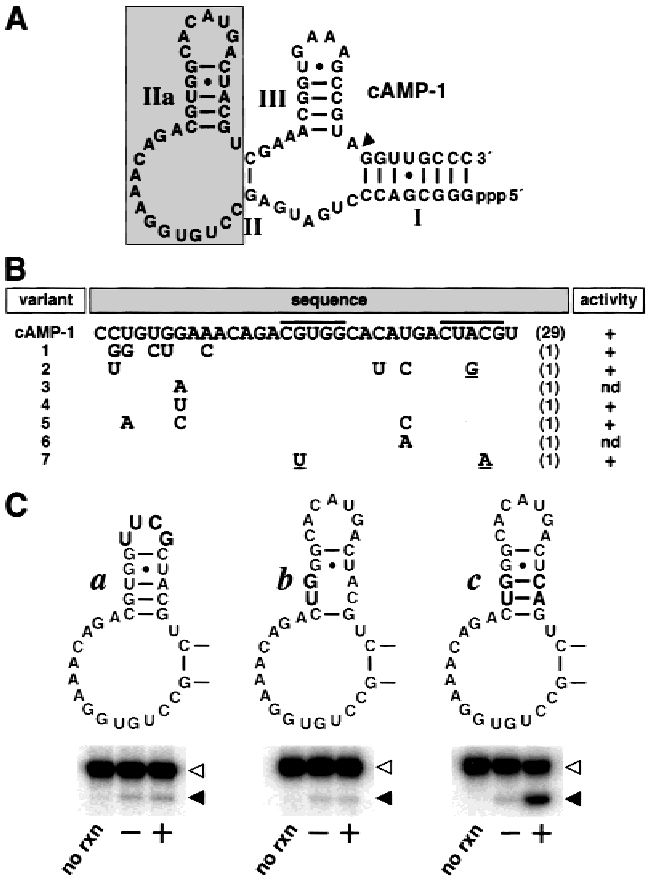

FIGURE 3. Secondary structure analysis of a cAMP-dependent ribozyme. **A:** Proposed secondary structure of cAMP-1. Denoted are stems I, II, and III of the hammerhead ribozyme domain, the site of catalytic cleavage (arrowhead), and stem IIa of the cAMP-binding domain (shaded). **B:** Artificial phylogenetic analysis of cAMP-1. Shown are sequence variants of cAMP-1 that were identified by allosteric selection for ligand-dependent function from a degenerate population of ribozymes. Annotations are as described for Figure 1B. **C:** Mutational analysis of cAMP-1. Shown are sequence variants of cAMP-1 (stem II region only) that examine different structural aspects of the ligand-binding domain. Annotations are as described for Figure 1C.

Disintegration of allosteric ribozyme domains

In several previous studies, preexisting aptamer and ribozyme domains were conjoined to create allosteric ribozymes (Soukup & Breaker, 2000b). The success of this engineering approach relies in part on the modular nature of certain RNA domains. Because the effector-binding components of the allosteric ribozymes described herein were made by allosteric selection, it cannot automatically be assumed that the capacities of these domains to bind their corresponding ligands will be retained when the ribozyme domain is removed.

To determine whether the effector-binding domains raised by allosteric selection exhibit modular characteristics, we employed a reverse engineering strategy to disintegrate the effector-binding and ribozyme domains from one another. In this approach, we assumed that the hammerhead ribozyme must form the single G-C base pair comprising stem II in order to exhibit self-cleavage activity. Because binding of the corresponding cNMP of each allosteric construct brings about the active state of the ribozyme, the ligand-bound form of the effector-binding domain must coexist with the stem II base pair. Furthermore, because the nucleotides forming the core of the hammerhead three-stem junction immediately adjacent to stem II are predicted to form a helix-like structure (Pley et al., 1994), we reasoned that the hammerhead domain could be replaced by a simple Watson–Crick base-paired element.

Using this rationale, we prepared three RNAs corresponding to the effector-binding domains of the cGMP-1, cCMP-1, and cAMP-1 ribozymes. RNAs representing only the ligand-binding domain from each allosteric ribozyme were transcribed, where stem II was extended by 5 bp to replace the ribozyme domain (Figs. 4A, 5A, and 6A). To address whether each domain can bind its cognate ligand when isolated from the allosteric ribozyme, the RNAs were examined for ligand-dependent conformational changes or induced fit characteristics (also called “adaptive binding”; Patel et al., 1997; Hermann & Patel, 2000). The susceptibility of the phosphodiester linkages of each RNA to spontaneous cleavage resulting from intramolecular transesterification was evaluated in the absence or presence of ligand. This structure-probing technique, previously used to investigate ligand-mediated changes in RNA conformation (Soukup & Breaker, 1999d), relies on the expectation that linkages constrained to a “non-in-line” orientation will exhibit low rates of spontaneous cleavage. In contrast, linkages located in relatively unstructured regions of RNA that are free to explore many conformational states will occasionally sample an “in-line” structure, which leads to an increased level of spontaneous cleavage. Therefore, ligand binding by RNAs that undergo a concomitant change in conformation can be observed by monitoring the changes in the rates of spontaneous transesterification throughout the polynucleotide.

The detached effector-binding domain from cGMP-1 RNA (Fig. 4A) exhibits relatively modest changes in the pattern resulting from spontaneous transesterification in response to ligand addition (Fig. 4B). The cleavage patterns for the detached cGMP-1 RNA in the presence of the noncognate cAMP or cCMP effectors (Fig. 4B, lanes 4 and 5, respectively) differ slightly from that observed in the absence of ligand (Fig. 4B, lane 6) in that there appears to be a general enhancement in cleavage rate. This suggests that high concentrations of noncognate ligands may have a nonspecific denaturing effect on the cGMP-binding RNA, or in some other way modestly accelerate RNA transesterification. In contrast, the cleavage pattern observed in the presence of cGMP (Fig. 4B, lane 12) demonstrates that cognate ligand has a stabilizing effect on RNA conformation. The effect is apparent, albeit only weakly, from cleavage rates of phosphodiester linkages throughout loop IIb (nt 27–33) and the loop regions comprising the three-stem junction (e.g., nt 20–23). Ligand-dependent changes in cleavage pattern are most notable at certain phosphodiester linkages such as those 3′ to nucleotides C7, C8, and C39. These data indicate that the detached cGMP-1 domain undergoes conformational changes specifically in the presence of cGMP that are consistent with adaptive binding. Furthermore, an analysis of cleavage at C39 in the presence of various concentrations of cGMP establishes a curve with which the apparent dissociation constant (K_d) can be determined (Fig. 4C). An apparent K_d was derived graphically by assuming that the fraction of RNA cleaved at position C39 is maximal in the presence of 10 μM cGMP and minimal in the presence of 10 mM cGMP (Fig. 4C, lanes 7 and 12, respectively). Therefore, the concentration of cGMP ($\sim$2 mM) that provides half-maximal cleavage at C39 reflects the apparent K_d for cGMP binding. The apparent K_d value of 2 mM for the cGMP-binding RNA is comparable to that previously determined for the allosteric ribozyme (Koizumi et al., 1999), suggesting that disintegration of the cGMP-binding domain from the original cGMP-1 allosteric ribozyme has not significantly altered its ability to bind cGMP. Similar results are obtained upon the analysis of other linkages whose cleavage is altered by the addition of cGMP (Fig. 4D).

It is important to note that ligand binding appears to stabilize an RNA structure that involves C39, which is positioned analogously to the cytosine residue that forms the single but critical G-C base pair in stem II of the cGMP-1 ribozyme. These data provide further evidence that the conformational changes accompanying cGMP binding ultimately serve to promote stem II formation, thereby revealing a likely mechanism for allosteric activation of the cGMP-1 ribozyme.

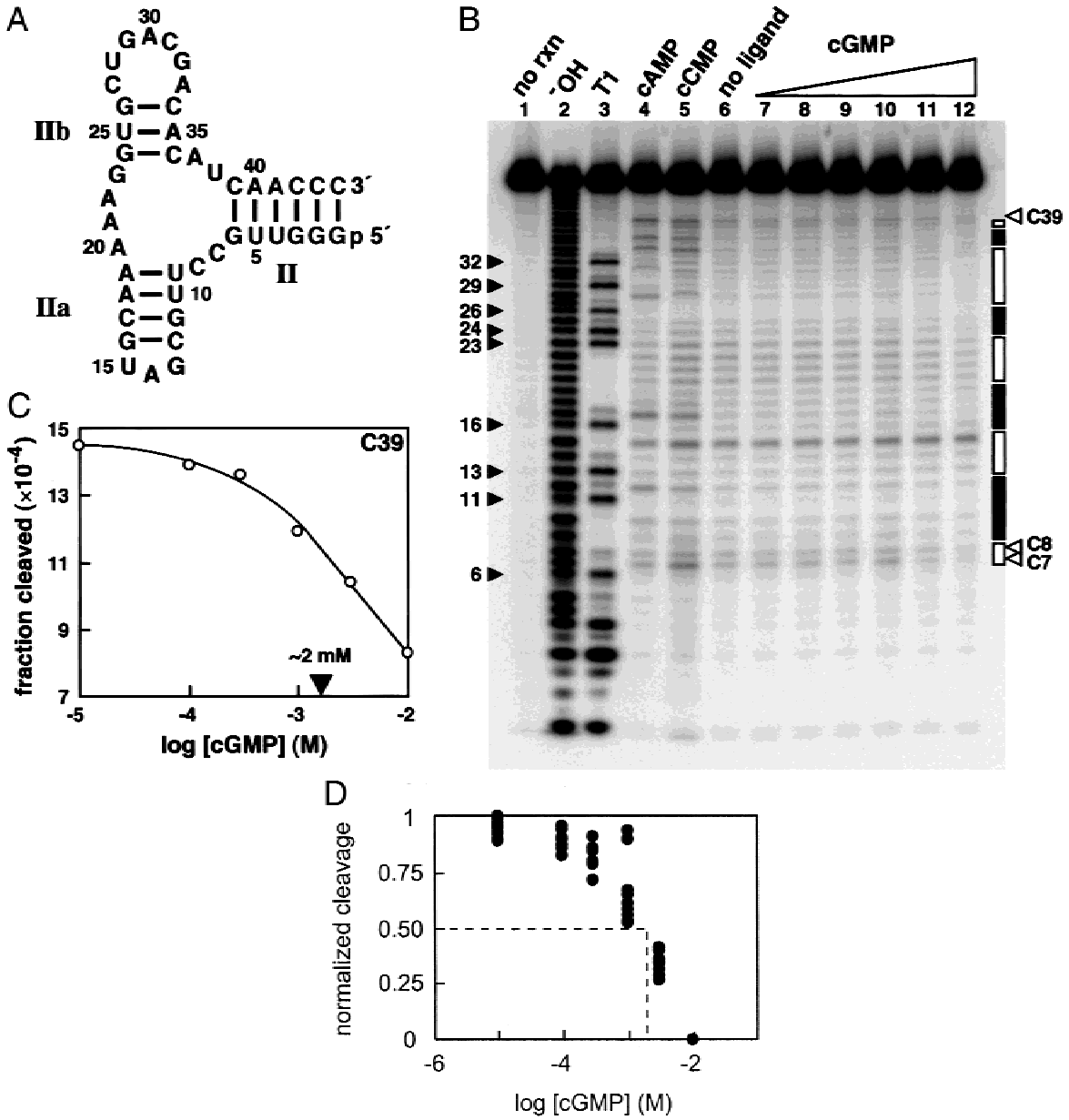

FIGURE 4. Structural analysis of the detached effector-binding domain of the cGMP-1 ribozyme. **A:** Sequence and proposed secondary structure of the effector-binding domain detached from cGMP-1. Nucleotides derived from the original effector-binding domain are indicated (bold). **B:** Uncatalyzed, ligand-dependent cleavage of the detached cGMP-1 domain by intramolecular phosphoester transfer. 5′-^{32}P-labeled RNA was incubated in selection buffer in the absence of ligand (lane 6) or in the presence of 10 mM cAMP (lane 4), 10 mM cCMP (lane 5), or various concentrations of cGMP (10 μM, 100 μM, 300 μM, 1 mM, 3 mM, or 10 mM; lanes 7–12, respectively). Cleavage products were separated by denaturing 10% PAGE. Also shown are unreacted RNA (lane 1) and RNA ladders generated by hydroxide-mediated cleavage (lane 2) and RNase T1 (G-specific cleavage; lane 3). Filled arrowheads identify bands corresponding to cleavage 3′ relative to guanosine residues. Open and filled boxes indicate putative loop and stem regions, respectively, of the detached RNA domain. Open arrowheads identify nucleotides at which the rate of spontaneous transesterification most notably changes with respect to ligand concentration. The gel image depicts the results of one of two replicate experiments that provided near identical results. **C:** Ligand-dependent phosphodiester cleavage at C39 of the cGMP-binding RNA. The fraction of RNA cleaved 3′ to C39 with respect to various concentrations of cGMP is plotted. The arrowhead denotes a minimum apparent dissociation constant of ~2 mM. **D:** Similar apparent K_d values are generated upon analysis of spontaneous cleavage, for example, at C7, C8, U9, A20, A21, G23, G24, and U25. Normalized cleavage values were established by the equation $(n - y)(m - y)^{-1}$, where n is the fraction of RNA cleaved at a given concentration of effector, m is the maximum value measured for fraction of RNA cleaved at a given site (typically obtained in the absence of effector), and y is the minimum value measured for fraction of RNA cleaved at this site (typically obtained in the presence of 10 mM effector). Dashed lines represent half-maximal cleavage and identify the K_d for effector binding as determined in **C**.

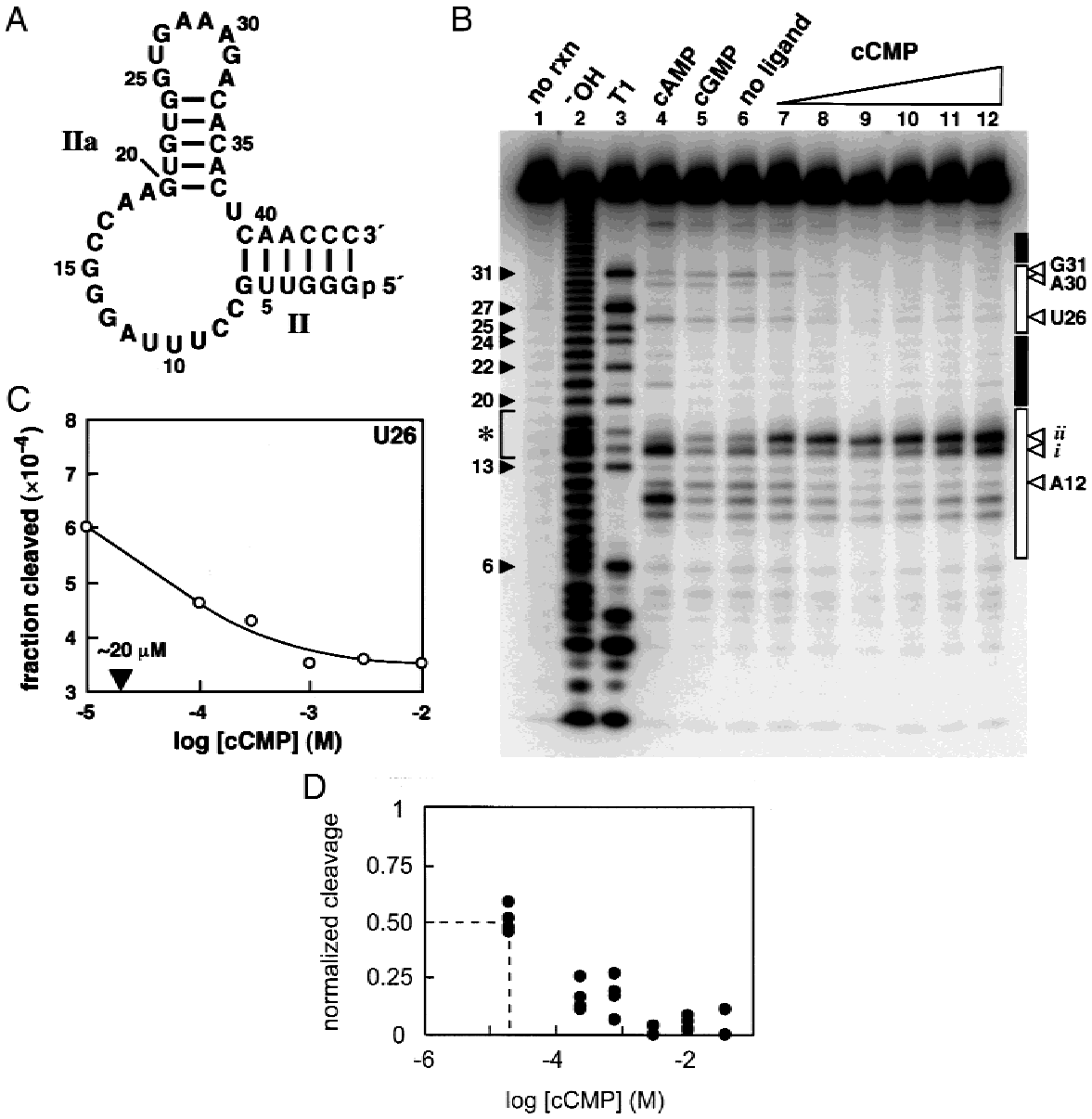

FIGURE 5. Structural analysis of the detached effector-binding domain of the cCMP-1 ribozyme. **A:** Sequence and proposed secondary structure of the effector-binding domain detached from cCMP-1. Nucleotides derived from the original effector-binding domain of cCMP-1 are indicated (bold). **B:** Uncatalyzed, ligand-dependent cleavage of the detached cCMP-1 domain by intramolecular phosphoester transfer. 5′-^{32}P-labeled RNA was incubated in selection buffer in the absence of ligand (lane 6) or in the presence of 10 mM cAMP (lane 4), 10 mM cGMP (lane 5), or various concentrations of cCMP (10 μM, 100 μM, 300 μM, 1 mM, 3 mM, or 10 mM; lanes 7–12, respectively). Cleavage products were separated by denaturing 10% PAGE. An asterisk denotes an unresolved region of compression between G13 and G20, within which nucleotides *i* and *ii* reside. Other annotations are as described for Figure 4B. **C:** Ligand-dependent phosphodiester cleavage at U26 of the detached domain from cCMP-1. The fraction of RNA cleaved 3′ to U26 with respect to various concentrations of cCMP is plotted. The arrowhead denotes an apparent dissociation constant of ~20 μM. **D:** Similar apparent K_d values are generated upon analysis of spontaneous cleavage, for example, at A12, A30, and G31. Details are as described in the legend to Figure 4D.

More obvious ligand-dependent cleavage patterns were observed for the detached effector-binding domains of cCMP-1 and cAMP-1 RNAs (Figs. 5B and 6B, respectively), indicating that these RNAs also undergo adaptive binding. For each detached effector-binding domain, ligand-dependent increases or decreases in cleavage rates were observed for certain linkages within the asymmetric bulge loop and loop IIa. For the cCMP-binding RNA, the most marked decreases in cleavage were observed for linkages 3′ to nucleotides A12, U26, A30, and G31, whereas increases in cleavage were noted at the unassigned positions *i* and *ii* (Fig. 5B,

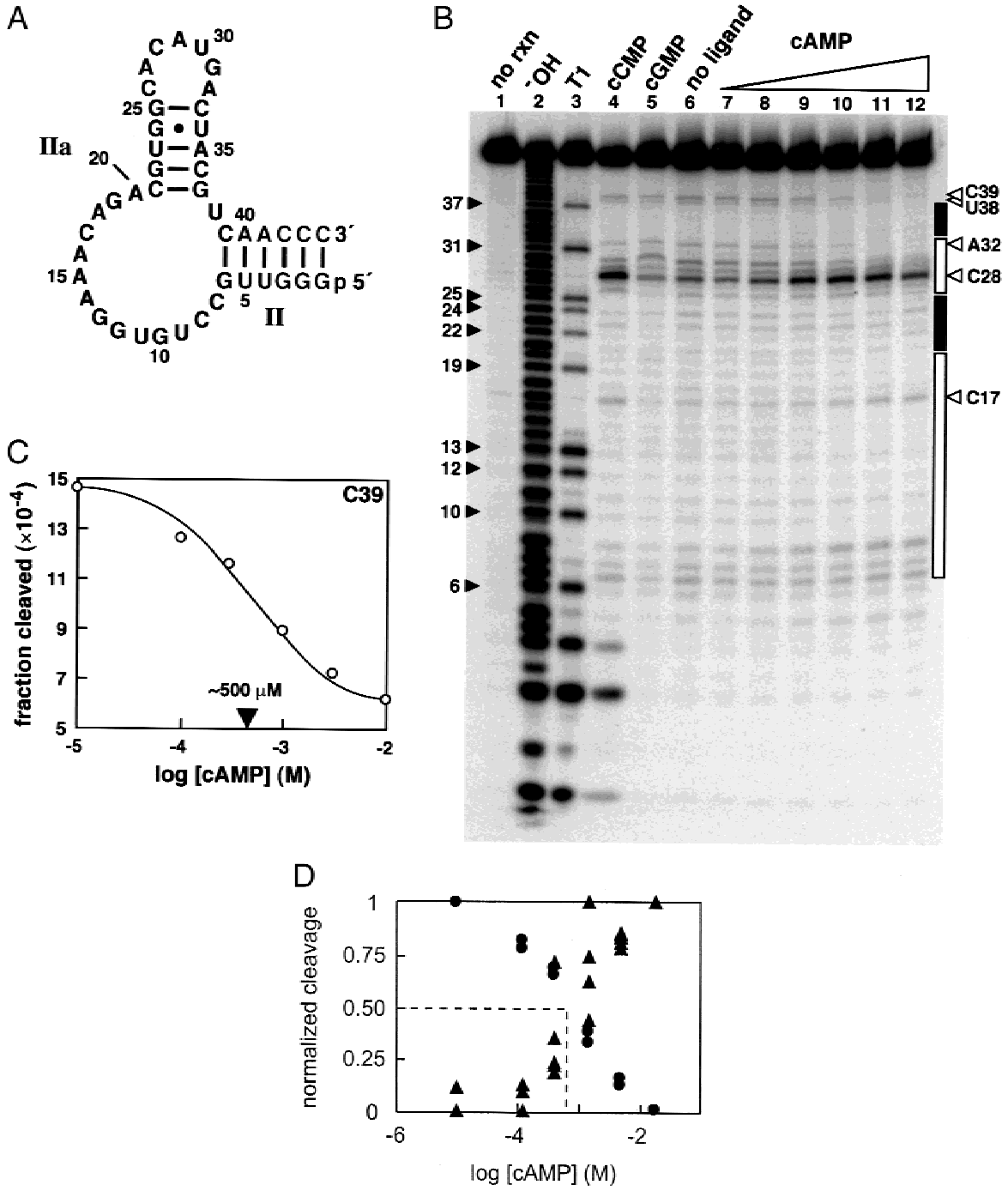

FIGURE 6. Structural analysis of the detached effector-binding domain of the cAMP-1 ribozyme. **A:** Proposed secondary structure of the effector-binding domain detached from cAMP-1. Nucleotides derived from the original effector-binding domain of cAMP-1 are indicated (bold). **B:** Uncatalyzed, ligand-dependent cleavage of the detached cAMP-1 domain by intramolecular phosphoester transfer. 5′-^{32}P-labeled RNA was incubated in selection buffer in the absence of ligand (lane 6) or in the presence of 10 mM cCMP (lane 4), 10 mM cGMP (lane 5), or various concentrations of cAMP (10 μM, 100 μM, 300 μM, 1 mM, 3 mM, or 10 mM; lanes 7–12, respectively). Cleavage products were separated by denaturing 10% PAGE. Other annotations are as described for Figure 4B. **C:** Ligand-dependent phosphodiester cleavage at C39 of the detached domain of the cAMP-1 RNA. The fraction of RNA cleaved 3′ to C39 with respect to various concentrations of cAMP is plotted. The arrowhead denotes an apparent dissociation constant of ~500 μM. **D:** Similar apparent K_d values are generated upon analysis of spontaneous cleavage for example at C7, C8, U9, C17, C28, A32, and U38. Details are as described in the legend to Figure 4D. Triangles identify data for linkages (C7, C8, U9, C17, and C28) that experience cleavage rate enhancement upon addition of effector. In these cases, the maximum value measured for fraction of RNA cleaved (m) at a given site typically is obtained in the presence of 10 mM of effector, and the minimum value measured for fraction of RNA cleaved (y) at this site typically is obtained in the absence of effector.

compare lanes 6–12). Further analysis of cleavage at U26 reveals that the detached domain from cCMP-1 RNA exhibits an apparent K_d of ~20 μM (Fig. 5C), representing an increase in ligand-binding affinity of ~150-fold relative to the cCMP-1 ribozyme (Koizumi et al., 1999). For the detached domain from cAMP-1, the most apparent ligand-dependent decreases in cleavage were observed for linkages 3′ to A32, U38, and C39, whereas increases in cleavage were noted at C17 and C28 (Fig. 6B, compare lanes 6–12). Cleavage at C39 demonstrates that the detached effector-binding domain from cAMP-1 has an apparent K_d of ~500 μM (Fig. 6C), which represents only a twofold increase in binding affinity relative to the cAMP-1 ribozyme (Koizumi et al., 1999). Similar dissociation constants were obtained by examining the effector-dependent cleavage patterns of other sites in the cCMP-1 and cAMP-1 RNAs (Figs. 5D and 6D).

Interestingly, ligand binding does not elicit the same structural stabilization of C39 in the detached cCMP-1 domain that was observed in the detached domains from the cGMP-1 and cAMP-1 RNAs. In addition, only the effector-binding domain from cCMP-1 exhibits a substantial improvement in K_d when examined separately from the ribozyme. It is possible that the detached cCMP domain is uniquely affected by the extra base pairs added to the stem II element, such that the critical G6-C39 base pair is stabilized even in the absence of its cCMP ligand. If this is the case, then the increase in apparent K_d observed for the cCMP-binding RNA could be attributed in part to the conformational preorganization of stem II (Van Duyne et al., 1991; Giebel et al., 1995; Katz, 1995; Sussman et al., 2000).

The cleavage patterns of the detached domains from cCMP-1 and cAMP-1 in the presence of noncognate ligands suggest that certain compounds might act as antagonists of cNMP-dependent ribozyme function. For example, the cleavage pattern observed for the cCMP-binding RNA in the presence of cAMP is similar to that evoked by cCMP (Fig. 5B, compare lanes 4, 6, and 12). Likewise, the cleavage pattern observed for the cAMP-binding RNA in the presence of cCMP resembles that elicited by the cognate ligand (Fig. 6B, compare lanes 4, 6, and 12). These data suggest that cAMP and cCMP might interact with the cCMP- and cAMP-binding RNAs, respectively, although neither noncognate ligand is capable of activating the respective allosteric ribozyme (Koizumi et al., 1999). To investigate whether cGMP, cCMP, or cAMP acts as an antagonist of cGMP-1, cCMP-1, or cAMP-1 ribozyme function, each ribozyme was assayed for activity in the presence of 500 μM cognate ligand in the absence or presence of 5 mM of either noncognate ligand. Only cCMP-1 was inhibited by noncognate ligand, exhibiting one-half the cCMP-dependent rate constant for self-cleavage in the presence of cAMP (data not shown).

Affinity maturation of a cNMP-dependent ribozyme

To address whether allosteric ribozymes that possess higher affinity binding sites for cNMP effectors can be developed, we sought to isolate variants that retain cNMP-dependent function under lower effector concentration using allosteric selection. The ligand-binding domains of several cNMP-dependent ribozymes were mutagenized to generate an initial population from which variants were selected for self-cleavage in the presence of cNMPs at one-tenth concentration (50 μM) relative to that which originally yielded the parent ribozymes (Koizumi et al., 1999). The reduction of effector concentration is expected to give those variant ribozymes with higher affinity binding sites a selective advantage. Eleven rounds of allosteric selection provided a final population of catalysts that exhibits markedly greater self-cleavage in the presence of cNMPs than in the absence of effectors (data not shown).

Sequence analysis revealed that the final population largely consists of variants of cGMP-1 (data not shown), the majority of which contain a subset of two specific mutations that replace the terminal A-U base pair in stem IIa with a G-C base pair. One clone containing only the two specific mutations (Fig. 7A) was analyzed in greater detail. The apparent K_d (~200 μM) for the cGMP-1 variant is approximately one-tenth of the value determined for the parental cGMP-1 RNA (Fig. 7B). The new G-C base pair present in the variant ribozyme could effect high-affinity binding by promoting preorganization of the effector-binding domain because it is expected to contribute greater thermodynamic stability to stem IIa (Serra & Turner, 1995). Alternatively, the terminal G-C base pair of stem IIa could more directly affect specific contacts between the RNA and bound effector. These data demonstrate that allosteric selection can be used to refine the binding characteristics of prototype allosteric ribozymes that are isolated from large populations of random-sequence RNAs.

DISCUSSION

Disintegration of ligand-binding and catalytic domains

The purposeful integration of well-characterized ligand binding and catalytic RNAs has been used to generate numerous allosteric ribozymes for which either precise or general mechanisms of allosteric regulation have been identified (Soukup & Breaker, 2000b). However, allosteric selection has made possible the isolation of novel effector-dependent nucleic acid catalysts for which neither the specifics of molecular recognition nor allosteric function are readily apparent (Koizumi et al., 1999). Undoubtedly, this combination of unknowns renders the detailed mechanisms of these allosteric catalysts less

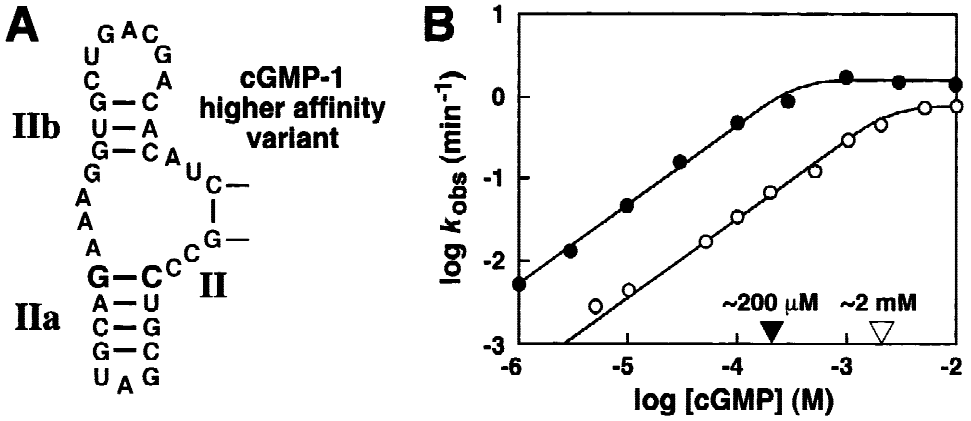

FIGURE 7. A higher affinity cGMP-dependent ribozyme identified by allosteric selection. **A:** Proposed secondary structure of a higher-affinity cGMP-1 variant. Shown is the stem II region only of a cGMP-1 variant containing two mutations (bold) relative to the parent construct. **B:** Ligand-binding affinities for cGMP-1 and the higher affinity variant. The logarithm of the observed rate constant versus the logarithm of cGMP concentration is plotted for cGMP-1 (open circles) and the higher affinity variant (filled circles). The apparent dissociation constants for cGMP-1 and the higher affinity variant indicated by the open and filled arrowheads, respectively, differ by one order of magnitude.

easily discernible. Nevertheless, it is possible to begin to understand certain aspects of molecular recognition and allosteric function through the use of RNA structure prediction algorithms, artificial phylogeny data, mutational analysis, and the separation of functional effector-binding and catalytic domains.

In this study, both computer-aided structure prediction and artificial phylogenies were used to examine three cNMP-dependent ribozymes isolated previously (Koizumi et al., 1999). The resulting secondary structure models have been further substantiated by mutational analysis. These studies delineate the requisite but sequence-insensitive secondary structure elements of each effector-binding domain, which serve to constrain the remaining nucleotides that are required for effector recognition and allosteric function.

For each cNMP-dependent ribozyme, the effector-binding domain is comprised of a two- or three-stem junction, where one stem (stem II) is formed from a single G-C base pair that is an essential feature of the active hammerhead ribozyme (Ruffner et al., 1990; Fedor & Uhlenbeck, 1992). In addition to the unpaired nucleotides that comprise the multistem junction, the composition of an adjacent loop region impacts the function of each allosteric ribozyme. Presently, it is unclear what specific interactions might exist between nucleotides that comprise the loop and those within the multistem junction. Furthermore, it is unknown whether either region might contribute more to effector recognition or to the structural dynamics that enable conformational transitions. Further insight regarding the function of these allosteric catalysts can be gained through bisection into distinct functional domains.

By definition, the effector-binding and catalytic sites of an allosteric enzyme are spatially distinct. Consequently, the functional domains of an allosteric catalyst are theoretically separable. The cNMP-binding domain from each allosteric ribozyme was prepared in isolation from the catalytic domain, and each was demonstrated to exhibit adaptive binding (Patel et al., 1997; Hermann & Patel, 2000) when incubated with its cognate ligand. These studies provide evidence that the effector-binding site of each allosteric ribozyme examined in this study is distinct from the adjacent ribozyme domain. Furthermore, assuming that the ligand-induced conformational changes exhibited by each cNMP-binding RNA are identical to those that contribute to allosteric activation of the corresponding ribozyme, a precise mechanism of allosteric regulation involving ligand-induced stabilization of the catalytically requisite G-C base pair in stem II can be corroborated. This work serves both to unravel the structure and function of the cNMP-dependent ribozymes, and to validate allosteric selection as a viable means of generating both interdependent and independent molecular recognition motifs that are similar to aptamers.

Affinity maturation of allosteric ribozymes

Any form of macromolecular combinatorial selection cannot help but to parallel the natural processes of the vertebrate immune system. Thus, in the same way that protein antibodies are improved by affinity maturation, higher affinity variants of allosteric nucleic acids can be created through a fundamentally similar process of mutation and selection. Indeed, mutagenization and reselection of cNMP-dependent ribozymes under conditions that favor the survival of variants that bind effector with higher affinity gave rise to a cGMP-dependent variant that exhibits a 10-fold improved affinity for its effector.

Although affinity maturation is not a novel process, these studies demonstrate an essential component of the engineering process needed to create highly proficient allosteric ribozymes that function as biosensors or as genetic control elements.

Unfortunately, the isolation of variant ribozymes possessing even greater affinity for their effector compounds was occluded by "selfish" molecules that survive the selection process using alternative strategies (data not shown), as was observed in the original selection (Koizumi et al., 1999). Although future methodology must strive to evade such catalysts, one must consider the possibility that high-affinity variants may be exceedingly rare in certain instances. Furthermore, the very nature of an allosteric catalyst may negatively impact its capacity for high-affinity molecular recognition. Specifically, the allosteric transition or conformational change that must accompany effector binding disallows the preformation of a well-ordered complementary binding surface for ligand recognition, which typically correlates with relatively higher affinity (Van Duyne et al., 1991; Giebel et al., 1995; Katz, 1995; Sussman et al., 2000). Aptamers that are generated by SELEX methods exhibit K_d values that usually range from ~10 mM to ~1 nM (Gold et al., 1995). It is therefore not surprising that the allosteric ribozymes examined in this study exhibit K_d values that are at the high end of this range (1–3 mM; Koizumi et al., 1999).

In dynamic molecular systems, the trade-off between the adaptive binding needed for allosteric function and the conformational preorganization needed for high-affinity binding must be overcome for extremely high-affinity effector recognition to be possible with allosteric ribozymes. In certain cases, removing the effector-binding domain from its parental allosteric construct can reduce this structural heterogeneity. For example, the ligand-binding affinity of the cCMP domain described in this study (Fig. 5) is improved by ~150 fold when removed from the cCMP-1 allosteric ribozyme. One possibility is that the extended stem II of the independent effector-binding domain serves to significantly preorganize the RNA, thereby improving its affinity for cCMP. In contrast, the cGMP- and cAMP-binding domains might not experience significant preorganization by extension of their respective stem II elements, and therefore do not exhibit improvements in ligand affinity. Consistent with this possibility is the observation that ligand binding to the cGMP- and cAMP-specific RNAs reduces spontaneous cleavage at nucleotide C39, whereas this same linkage in the cCMP-binding RNA is resistant to cleavage even in the absence of ligand. Perhaps the stem II extensions of the cGMP and cAMP RNAs are insufficient to stabilize the critical G8-C39 base pair of these RNAs, which otherwise would provide an improvement in binding affinity like that observed with the cCMP RNA.

CONCLUSIONS

Our extended analyses of the cNMP-dependent ribozymes reveal several fundamental properties of these allosteric catalysts and of the allosteric selection process. In each case, the effector-binding domain of the allosteric ribozyme is physically and functionally separable from the catalytic domain. The disintegration of independent ligand recognition motifs from allosteric ribozymes validates allosteric selection as a means of concurrently generating novel aptamer-like domains for multiple compounds in a rapid manner. These findings further reveal the modular nature of RNA structures. In addition, the ligand-binding affinity of an allosteric ribozyme can be improved through mutagenization and reselection under conditions that favor tighter binding. Affinity maturation in this sense will likewise prove to be a valuable attribute of allosteric selection as future endeavors seek to apply allosteric ribozymes as biosensors and genetic switches.

MATERIALS AND METHODS

Preparation of RNA

RNAs were transcribed from double-stranded DNAs using T7 RNA polymerase. Double-stranded DNAs were generated by reverse transcriptase (RT) extension of primer 1 (5′-TAA TACGACTCACTATAG) or primer 2 (5′-TAATACGACTCACT ATAGGGCGACCCTGATGAG) using synthetic DNA templates complementary to the desired RNA. Synthetic DNAs were prepared by standard solid phase methods (Keck Biotechnology Resource Laboratory, Yale University) and purified by denaturing (8 M urea, 89 mM Tris base, 89 mM boric acid, 1 mM EDTA) 10% polyacrylamide gel electrophoresis (PAGE), crush-soak elution (in 10 mM Tris-HCl [pH 7.5 at 23 °C], 200 mM NaCl, 1 mM EDTA), and precipitation with ethanol. RT extension reactions (50 μL) containing 200 pmol template DNA, 300 pmol primer DNA, 50 mM Tris-HCl (pH 8.3 at 23 °C), 75 mM KCl, 3 mM $MgCl_2$, 1 mM DTT, 1 mM each dNTP, and 400 U SuperScript II reverse transcriptase (Gibco BRL) were incubated at 37 °C for 30 min. Extension products were precipitated with ethanol and redissolved in water. Transcription reactions (50 μL) containing ~40 pmol extension product, 40 mM Tris-HCl (pH 8.0 at 23 °C), 15 mM $MgCl_2$, 5 mM DTT, 50 μg/mL BSA, 1 mM each NTP, and ~1,000 U T7 RNA polymerase were incubated at 37 °C for 1 h. RNAs were purified by denaturing 10% PAGE. When necessary, RNAs were ^{32}P-labeled by supplementing transcription reactions with 3.3 pmol [α-^{32}P]-UTP (20 μCi). RNA populations were initially derived from DNA templates containing a degeneracy of 0.135 (86.5% wild type) per nucleotide position corresponding to the effector-binding domain of the ribozyme.

Artificial phylogenetic and mutational analyses of cNMP-dependent ribozymes

Artificial phylogenetic data were generated by allosteric selection for cNMP-dependent ribozyme function from degen-

erate RNA populations based on the cGMP-1, cCMP-1, or cAMP-1 ribozymes (Koizumi et al., 1999). Each round of allosteric selection consisted of preselection against cNMP-independent self-cleavage activity and selection for cNMP-dependent self-cleavage activity. Selected RNAs were reverse transcribed, and their cDNA products were amplified by PCR to produce templates for the transcription of subsequent RNA populations using T7 RNA polymerase. For the initial round of selection, 28 pmol each RNA population (84 pmol total RNA, 5×10^{13} molecules) were incubated for 5 h at 23 °C in a reaction mixture (20 μL) containing selection buffer (50 mM Tris-HCl [pH 7.5 at 23 °C], 20 mM $MgCl_2$). The reaction was punctuated at 1 h intervals by incubation at 90 °C for 30 s. The uncleaved fraction of the population was isolated by denaturing 10% PAGE and subsequently incubated for 15 min at 23 °C in a reaction mixture (20 μL) containing selection buffer and 500 μM each cGMP, cCMP, and cAMP (Sigma). The cleaved fraction of the population was isolated by denaturing 10% PAGE. Cleavage reactions were terminated by the addition of an equal volume of gel loading buffer A (89 mM Tris base, 89 mM boric acid, 7.3 M urea, 40 mM EDTA, 20% sucrose, 0.1% SDS, 0.02% xylene cyanol, and 0.02% bromophenyl blue). RT reactions (40 μL) containing selected RNAs, 100 pmol primer 3 (5′-GGGCAACCTACGGCTTTCACCG TTTCG), 50 mM Tris-HCl (pH 8.3 at 23 °C), 75 mM KCl, 3 mM $MgCl_2$, 1 mM DTT, 0.4 mM each dNTP, and 400 U SuperScript II reverse transcriptase (Gibco BRL) were incubated at 37 °C for 30 min. PCR reactions (100 μL) containing half of the cDNA products, 100 pmol each primer 2 and primer 3, 10 mM Tris-HCl (pH 8.3 at 23 °C), 50 mM KCl, 1.5 mM $MgCl_2$, 0.01% gelatin, 0.2 mM each dNTP, and 5 U *Taq* DNA polymerase were thermocycled for the appropriate number of iterations at 94 °C for 30 s, 55 °C for 30 s, and 72 °C for 60 s. In two subsequent rounds of allosteric selection, 16.6 pmol (10^{13} molecules) of RNA were similarly manipulated. However, in the third and final round, three individual populations were selected for only cGMP-, cCMP-, or cAMP-dependent function. DNA corresponding to individual RNAs from the final populations was isolated using a TOPO TA Cloning Kit (Invitrogen) and was sequenced using a Thermo Sequenase Cycle Sequencing Kit (USB).

Sequence variants of the cGMP-1, cCMP-1, and cAMP-1 ribozymes were prepared either by PCR amplification from plasmid DNAs using primers 2 and 3, or from the appropriate synthetic DNA templates. Trace amounts (~100 nM) of ^{32}P-labeled sequence variants were assayed for cNMP-dependent self-cleavage activity by incubation at 23 °C for 15 min in the absence or presence of 500 μM cGMP, cCMP, or cAMP in selection buffer. Reactions were terminated by the addition of an equal volume of gel loading buffer A and the products were separated by denaturing 10% PAGE and visualized using a PhosphorImager and ImageQuant software (Molecular Dynamics).

Structural analysis of cNMP-binding RNAs

RNA structural analysis was similarly performed as previously described (Soukup & Breaker, 1999d). Prior to analysis, RNAs were dephosphorylated using calf intestinal alkaline phosphatase (CIAP; Roche Molecular Biochemicals) and 5′-^{32}P-labeled using T4 polynucleotide kinase (T4 PNK; New England Biolabs). Phosphatase reactions (20 μL) containing ~50 pmol RNA, 50 mM Tris-HCl (pH 8.5 at 20 °C), 100 μM EDTA, 2 U CIAP were incubated at 50 °C for 1 h. Dephosphorylated RNA was precipitated with ethanol and redissolved in water. Kinase reactions (20 μL) containing ~10 pmol dephosphorylated RNA, 70 mM Tris-HCl (pH 7.6 at 25 °C), 10 mM $MgCl_2$, 5 mM DTT, 10 pmol [γ-^{32}P]-ATP (60 μCi), and 20 U T4 PNK were incubated at 37 °C for 1 h. End-labeled RNAs were purified by denaturing 10% PAGE, isolated from the gel by crush-soak elution, precipitated with ethanol, redissolved in water, and quantitated by scintillation counting.

Trace amounts of 5′-^{32}P-labeled RNAs (~200 fmol) were incubated at 23 °C for precisely 48 h in the absence or presence of various concentrations of cGMP, cCMP, or cAMP in reactions (10 μL) containing selection buffer. Reactions were terminated by the addition of 15 μL water and 25 μL gel loading buffer B (10 M urea and 1.5 mM EDTA). RNA ladders were prepared essentially as previously described (Knapp, 1989). Briefly, hydroxide cleavage ladders were generated by incubating ~200 fmol RNA in reactions (10 μL) containing 50 mM $NaHCO_3$/Na_2CO_3 (pH 9.0 at 23 °C) and 1 mM EDTA for 7 min at 90 °C. G-specific sequencing ladders were generated by incubating ~200 fmol RNA in reactions (10 μL) containing 25 mM sodium citrate (pH 5.0 at 23 °C), 7 M urea, 1 mM EDTA, and 1 U RNase T1 (Roche Molecular Biochemicals) for 15 min at 55 °C. Reactions were quenched on ice and combined with 15 μL water and 25 μL gel loading buffer B. Reaction products separated by denaturing 10% PAGE were visualized and quantitated using a PhosphorImager and ImageQuant software (Molecular Dynamics). For each RNA, cleavage 3′ to each nucleotide position derived from the ligand-binding domain was examined. The fraction of total RNA cleaved at each nucleotide position was calculated.

Allosteric selection for higher affinity cNMP-dependent ribozymes

Allosteric selection for higher affinity cNMP-dependent ribozymes was performed as described herein. However, degenerate RNA populations based on the cGMP-1, cGMP-4, cCMP-1, cCMP-2, cAMP-1, or cAMP-2 ribozymes (Koizumi et al., 1999) were selected for function under reduced cNMP concentration (50 μM each cGMP, cCMP, and cAMP). Selection reactions were incubated for either 5 or 1 min. Individual members were isolated from the final population, sequenced, and assayed for cNMP-dependent self-cleavage activity.

Observed rate constants (k_{obs}) for cNMP-dependent ribozyme self-cleavage were established by plotting the natural logarithm of the fraction of substrate uncleaved versus time, where k_{obs} is derived as the negative slope of the resulting line. Trace amounts (~25 nM) of ^{32}P-labeled RNA were incubated at 23 °C in selection buffer containing various concentrations of cGMP in the range from 1 μM to 10 mM. Reactions were terminated by the addition of an equal volume of gel loading buffer A and the products were separated by denaturing 10% PAGE, and visualized and quantitated using a PhosphorImager and ImageQuant software (Molecular Dynamics).

ACKNOWLEDGMENTS

We thank members of the Breaker Laboratory for helpful discussions and T. D'Onofrio for contributions to sequence

analysis. This work was supported by research grants from the National Institutes of Health (GM559343), the Defense Advanced Research Projects Agency (DARPA), and the Yale Diabetes Endocrine Research Center (DERC). Support was also provided by fellowships to R.R.B. from the Hellman Family and from the David and Lucile Packard Foundation.

Received November 24, 2000; returned for revision December 21, 2000; revised manuscript received January 9, 2001

REFERENCES

Araki M, Okuno Y, Hara Y, Sugiura Y. 1998. Allosteric regulation of a ribozyme activity through ligand induced conformational change. *Nucleic Acids Res 26*:3379–3384.

Breaker RR. 1997. In vitro selection of catalytic polynucleotides. *Chem Rev 97*:371–390.

Carola C, Eckstein F. 1999. Nucleic acid enzymes. *Curr Opin Chem Biol 3*:274–283.

Chow CS, Bogdan FM. 1997. A structural basis for RNA-ligand interactions. *Chem Rev 97*:1489–1513.

Eckstein F, Lilley DMJ, eds. 1996. *Catalytic RNA*. Berlin: Springer-Verlag.

Famulok M. 1999. Oligonucleotide aptamers that recognize small molecules. *Curr Opin Struct Biol 9*:324–329.

Fedor MJ, Uhlenbeck OC. 1992. Kinetics of intermolecular cleavage by hammerhead ribozymes. *Biochemistry 31*:12042–12054.

Giebel LB, Cass R, Milligan DL, Young D, Arze R, Johnson C. 1995. Screening of cyclic peptide phage libraries identifies ligands that bind streptavidin with high affinities. *Biochemistry 34*:15430–15435.

Gold L, Polinsky B, Uhlenbeck OC, Yarus M. 1995. Diversity of oligonucleotide functions. *Annu Rev Biochem 64*:763–797.

Hamada M, Kuwabara T, Warashina M, Nakayama A, Taira K. 1999. Specificity of novel allosterically *trans*- and *cis*-activated connected maxizymes that are designed to suppress *BCR-ABL* expression. *FEBS Lett 461*:77–85.

Hermann T, Patel DJ. 2000. Adaptive recognition by nucleic acid aptamers. *Science 287*:820–825.

Hertel KJ, Pardi A, Uhlenbeck OC, Koizumi M, Ohtsuka E, Uesugi S, Cedergren R, Eckstein F, Gerlach WL, Hodgson R. 1992. Numbering system for the hammerhead. *Nucleic Acids Res 20*:3252.

Jose AM, Soukup GA, Breaker RR. 2001. Cooperative binding of effectors by an allosteric ribozyme. *Nucleic Acids Res*: in press.

Katz BA. 1995. Binding to protein targets of peptidic leads discovered by phage display: Crystal structures of streptavidin-bound linear and cyclic peptide ligands containing the HPQ sequence. *Biochemistry 34*:15421–15429.

Knapp G. 1989. Enzymatic approaches to probing of RNA secondary and tertiary structure. *Methods Enzymol 180*:192–212.

Koizumi M, Soukup GA, Kerr JNQ, Breaker RR. 1999. Allosteric selection of ribozymes that respond to the second messengers cGMP and cAMP. *Nat Struct Biol 6*:1062–1071.

Komatsu Y, Yamashita S, Kazama N, Nobuoka K, Ohtsuka E. 2000. Construction of new ribozymes requiring short regulator oligonucleotides as a cofactor. *J Mol Biol 299*:1231–1243.

Kuwabara T, Warashina M, Tanabe T, Tani K, Asano S, Taira K. 1998. A novel allosterically *trans*-activated ribozyme, the maxizyme, with exceptional specificity in vitro and in vivo. *Molecular Cell 2*:617–627.

Long DM, Uhlenbeck OC. 1994. Kinetic characterization of intramolecular and intermolecular hammerhead RNAs with stem II deletions. *Proc Natl Acad Sci USA 91*:6977–6981.

Osborne SE, Ellington AD. 1997. Nucleic acid selection and the challenge of combinatorial chemistry. *Chem Rev 97*:349–370.

Patel DJ, Suri AK, Jiang F, Jiang L, Fan P, Kumar RA, Nonin S. 1997. Structure, recognition and adaptive binding in RNA aptamer complexes. *J Mol Biol 272*:645–664.

Pley HW, Flaherty KM, McKay DB. 1994. Three-dimensional structure of a hammerhead ribozyme. *Nature 372*:68–74.

Porta H, Lizardi PM. 1995. An allosteric hammerhead ribozyme. *Biotechnol 13*:161–164.

Robertson MP, Ellington AD. 1999. In vitro selection of an allosteric ribozyme that transduces analytes to amplicons. *Nat Biotechnol 17*:62–66.

Robertson MP, Ellington AD. 2000. Design and optimization of effector-activated ribozyme ligases. *Nucleic Acids Res 28*:1751–1759.

Ruffner DE, Stormo GD, Uhlenbeck OC. 1990. Sequence requirements of the hammerhead RNA self-cleavage reaction. *Biochemistry 29*:10695–10702.

Seetharaman S, Zivarts M, Sudarsan N, Breaker RR. 2001. Immobilized RNA switches for the analysis of complex chemical and biological mixtures. *Nature Biotechnol*: in press.

Serra MJ, Turner DH. 1995. Predicting thermodynamic properties of RNA. *Methods Enzymol 259*:242–261.

Soukup GA, Breaker RR. 1999a. Nucleic acid molecular switches. *Trends Biotechnol 17*:469–476.

Soukup GA, Breaker RR. 1999b. Design of allosteric hammerhead ribozymes activated by ligand-induced structure stabilization. *Structure 7*:783–791.

Soukup GA, Breaker RR. 1999c. Engineering precision RNA molecular switches. *Proc Natl Acad Sci USA 96*:3584–3589.

Soukup GA, Breaker RR. 1999d. Relationship between internucleotide linkage geometry and the stability of RNA. *RNA 5*:1308–1325.

Soukup GA, Breaker RR. 2000a. Allosteric nucleic acid catalysts. *Curr Opin Struct Biol 10*:318–325.

Soukup GA, Breaker RR. 2000b. Allosteric ribozymes. In: Krupp G, Gaur RK, eds. *Ribozyme biochemistry and biotechnology*. Natick, Massachusetts: Eaton Publishing. pp 149–170.

Soukup GA, Emilsson GAM, Breaker RR. 2000. Altering molecular recognition of RNA aptamers by allosteric selection. *J Mol Biol 298*:623–632.

Sussman D, Nix JC, Wilson C. 2000. The structural basis for molecular recognition by the vitamin B_{12} RNA aptamer. *Nature Struct Biol 7*:53–57.

Tanabe T, Takata I, Kuwabara T, Warashina M, Kawasaki H, Tani K, Ohta S, Asano S, Taira K. 2000. Maxizymes, novel allosterically controllable ribozymes, can be designed to cleave various substrates. *Biomacromolecules 1*:108–117.

Tang J, Breaker RR. 1997a. Rational design of allosteric ribozymes. *Chem Biol 4*:453–459.

Tang J, Breaker RR. 1997b. Examination of the catalytic fitness of the hammerhead ribozyme by in vitro selection. *RNA 3*:914–925.

Tang J, Breaker RR. 1998. Mechanism for allosteric inhibition of an ATP-sensitive ribozyme. *Nucleic Acids Res 26*:4222–4229.

Tuschl T, Eckstein F. 1993. Hammerhead ribozymes: Importance of stem-loop II for activity. *Proc Natl Acad Sci USA 90*:6991–6994.

Van Duyne GD, Standaert RF, Karplus PA, Schreiber SL, Clardy J. 1991. Atomic structure of FKBP-FK506, an immunophilin-immunosuppressant complex. *Science 252*:839–852.

Williams KP, Bartel DP. 1996. In vitro selection of catalytic RNA. *Nucleic Acids Mol Biol 10*:367–381.

Zuker M. 1989. On finding all suboptimal foldings of an RNA molecule. *Science 244*:48–52.